XIII International Conference on Computational Plasticity. Fundamentals and Applications
COMPLAS XIII
E. Oñate, D.R.J. Owen, D. Peric & M. Chiumenti (Eds)

MODELLING HOT LEVELLING PROCESSES BY UTILISING ARBITRARY LAGRANGIAN EULERIAN (ALE) CONCEPTS

CHRISTIAN WÖCKINGER*, ERIK PARTEDER†, ALEXANDER J. KAINZ‡ AND KLAUS ZEMAN‡

*Linz Center of Mechatronics (LCM)
Altenberger Straße 69, 4040 Linz, Austria
e-mail: christian.woeckinger@lcm.at - web page: http://www.lcm.at

†voestalpine Grobblech GmbH
voestalpine-Straße 3, 4020 Linz, Austria
e-mail: erik.parteder@voestalpine.com - web page: http://www.voestalpine.com/grobblech

‡Institute of Mechatronic Design and Production (IMDP), Johannes Kepler University Linz
Altenberger Straße 69, 4040 Linz, Austria
e-mail: alexander.kainz@jku.at, klaus.zeman@jku.at - web page: http://www.jku.at/imdp

Key words: Metal Forming, Hot Levelling, Heavy Plate, Arbitrary Lagrangian Eulerian

Abstract. During production of heavy plate, hot levelling is representing an important process step. The ability of simulating the production process including the influence of process parameters on product properties enables to track, guide and control crucial product properties, which is indispensable for modern production lines. The developed system of mathematical modelling components constitutes the basis for overcoming existing shortcomings by a new generation of off-line process models. Eliminating curvature and warping of flat products, caused by preceding production steps is the main purpose of all levelling technologies (e.g. hot and cold levelling and also tension levelling in strip production) and is achieved through repeated alternate bending of heavy plate around multiple levelling rolls, which additionally minimises residual stress. To identify and fully understand the underlying physical effects, *Abaqus*™ was employed for modelling and analysing the levelling process. Referential data obtained so far from systematic parametric studies form a well founded basis regarding subsequent model reduction techniques. The general-purpose concept and the primarily *Lagrangian* formulation of commerical FEM packages in combination with the highly non-linear characteristics of frictional contact, material and geometry may lead to extremely high computational costs. To overcome this problem, customized 2D plane strain models based on the principle of virtual work and a specialised steady-state ALE formalism in conjunction with "Parametric Shape Functions" describing relevant degrees of freedom of the deformed plate are derived, which yield key results like the bending-line and levelling forces.

1 INTRODUCTION & STATE OF THE ART

At first sight, heavy plate is a geometrically uncomplex, large-area, flat product haracterised by thickness, width and length. As a main provider of high quality niche products for the energy market, *voestalpine Grobblech GmbH* produces thermomechanically rolled plates for offshore wind parks, linepipe steels for sour service and high toughness steels for cryogenic temperatures applied for liquefied natural gas tankers. To track, guide and control crucial product properties throughout the whole production process contributes to satisfaction of customer demands. The heavy plate production line at *voestalpine Grobblech GmbH* (Figure 1) comprises two pusher furnaces and some pit furnaces for reheating slabs coming from the casting line, a quarto reversing roll stand with a subsequent accelerated cooling device, a hot leveller as well as a cold leveller (Figure 2). The main purpose of levelling as one of the main production steps is the elimination of plate curvature and warping due to the preceding production steps of rolling and rapid cooling.

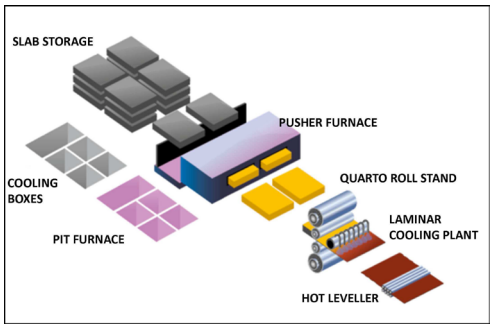

Figure 1: Heavy Plate Production Line

Figure 2: Hot Leveller

The principle of levelling is based upon repeated alternate bending of the plate around rotating levelling rolls (cp. Figure 3). To force the plate to bend around the rolls, the upper machine frame containing four rolls is moved downwards and skewed according to appropriate machine control parameters. Well known empirical strategies postulate an initial plastic bending imposing a well defined amount of curvature on the plate within the first section of the hot leveller (i.e. Roll 1 to 3 in Figure 3) that should eliminate all initially existing flatness errors including warping and waviness (in particular edge- and center-buckles). Based on this known state, the plate curvature is selectively reduced step by step with each following alternate plastic bending deformation in order to reach zero urvature, i.e. perfect flatness after levelling.

Early observations of levelling aimed at detecting and determining the maximum roll loads of the machine [1], which is important for dimensioning and construction of hot levellers. Efforts to analytically describe the plate's bending-line can be considered as first attempts to gather a well founded and deepened knowledge of the process itself [2]. Some crucial aspects of the forming process inside the hot leveller, in particular the repeated alternate plastic bending as well as a first rough estimate of the location

of contact points between plate and rolls were carried out analytically [3]. Usage of computers led to a deeper insight into the stress and strain distributions during forming of heavy plate [4]. To validate their respective results, some authors [3, 5] carried out experiments at trial rigs, which were progressively substituted by numerical simulations using commercial FEM-packages like *Abaqus*™ [6]. At IMDP a self-developed simulation prototype for a tension levelling process has been developed [7] during the last years.

2 MACHINE MODELS

As is well known from practical experience with hot levellers at production lines the levelling rolls, the machine frame and its components as well as the adjustment mechanism deform considerably under the occurring heavy loads [8]. The influence of levelling forces on machine deformation and feedback on the plate's bending-line cannot be neglected. In particular, the machine deformation has an impact on the center positions of the four upper levelling rolls. Hence, the actual positions $\boldsymbol{x}_{M,i}$ of roll centers in the loaded case will not coincide with the desired positions $\bar{\boldsymbol{x}}_{M,i}$ according to parameters `gap` and `skew` for the unloaded ase as represented in Figure 3.

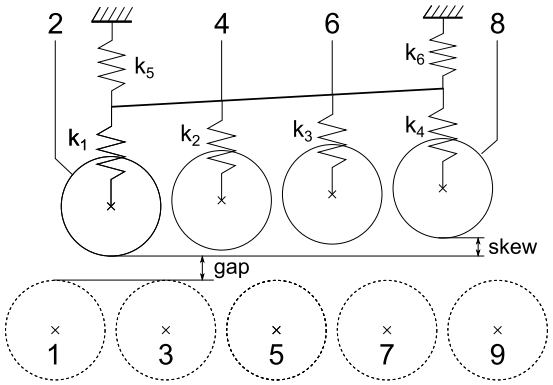

Figure 3: Geometry of a hot leveller with machine frame stiffness

Roll displacements $\boldsymbol{u} = \boldsymbol{x}_{M,i}(\boldsymbol{F}) - \bar{\boldsymbol{x}}_{M,i}$ and levelling forces $\boldsymbol{F}$ are connected by a matrix $\boldsymbol{K}_{MRig}$ representing machine rigidity whose matrix components K_{ij} can be represented as linear combinations of single spring stiffness values k_l, $l \in [1, 6]$ as shown in Figure 3, hence $\boldsymbol{u}(\boldsymbol{F}) = \boldsymbol{K}_{MRig}^{-1} \cdot \boldsymbol{F}$ yields roll displacements subject to levelling forces. Actual levelling roll positions $\boldsymbol{x}_{M,i}$ are therefore calculated from the desired roll positions $\bar{\boldsymbol{x}}_{M,i}$ and roll displacements $\boldsymbol{u}$. Via non-penetration constraints taken into account by *Lagrange* multiplier techniques (cp. (18)), the machine stiffness is easily incorporated into the tangential stiffness matrix for the highly non-linear overall system including the elasto-plastically deformed plate.

3 PROCESS MODEL USING COMMERCIAL FEM PACKAGES

It is considered to be state of the art to use commercial FEM packages as starting point for developing taylor-made process models, because neither can curvature, stresses and strains be measured online during processing, nor it is currently possible to test material properties of the final product non-destructively. Thus a mathematical description of such a process is an adequate approach to gain information regarding states and properties of the plate. Due to the general formulation of finite elements used in commercial, general-purpose FEM packages they are applicable to a variety of metal forming problems, which

is used to identify and fully understand the underlying physical effects. However, the flexibility of these packages in combination with primarily *Lagrangian* formalisms lead to high computational costs making such models unsuitable for extensive parametric studies. Therefore, a taylor-made formulation of the problem has been elaborated by model reduction techniques from the information gathered from general-purpose reference models.

Levelling rolls are modelled as 2D analytic rigid circular arcs. At the beginning of the numerical simulation, the upper levelling rolls are horizontally arranged in contact with an undeformed horizontal plate. A prescribed rigid body movement of the four upper rolls leads to final roll-center positions, defined by the parameters `gap` and `skew` (cp. Figure 3). The heavy plate is simulated within the frame of plane strain and is represented geometrically by a rectangular plane of given length and prescribed undeformed thickness. Due to the severe non-linearity of the problem resulting from contact, friction and non-linear path-dependent, elasto-plastic constitutive laws, even the 2D plane-strain FEM-models lead to unacceptably high run-times of several days.

The drive concept of the machine is based on controlling the driving torques of the rolls individually, hence in the numerical simulation model, the boundary conditions at the rolls are prescribed torques as time functions. Hence, the angular velocities of all levelling rolls can adjust kinematically fully independently from each other as part of the solution. A torque controller is realised by employing the *Abaqus*™ User Subroutine `VUAMP` enabling detailed corrective actions onto the model during the simulation process.

The *Abaqus*™ model of the levelling process, as pointed out above, was validated against data from an actual production process. Extensive parameter studies were carried out for varying plate thickness and roll setup (`gap`, `skew`). Automated generation of 2D plane strain models in *Abaqus*™ CAE using *Python*® scripts proved convenient for effective operation of such parameter studies that require a multitude of similar models.

Resultant data form a well founded basis for a hierarchical modelling approach to derive a self-developed customized software prototype by model reduction techniques to overcome the high computational costs of commercial general-purpose FEM simulation models.

4 PARAMETRIC SHAPE FUNCTION (PSF) MODEL

As the concept of PSF turned out to be very efficient for the class of tension levelling simulations under consideration [7], it is also applied here to form the basis for a software prototype of hot and cold levelling. Previously identified essential kinematic d.o.f. are approximated with linear shape functions regarding the plate's bending-line, the cross sectional strain distribution as well as shear strains, the latter of which is essential for thick plate (e.g. $H > 50\,\mathrm{mm}$). By utilising ALE (Arbitrary *Lagrangian Eulerian*) theory and an optimised non-equidistant element node distribution, simulation run-times could be reduced drastically compared to commercial FEM packages, whereas the quality of simulation results is almost equivalent.

5 ALE FORMALISM

There are two basic continuum-mechanical approaches. The *Lagrangian* material formulation considers a nodal mesh fixed to material particles, while the *Eulerian* spatial formulation investigates the spatial velocity field on a spatially-fixed mesh within an *Eulerian* "window" (cp. Figure 5), without considering every particle's path. Thereby the *Eulerian* and *Lagrangian* frames of reference are related by the time-dependent mapping

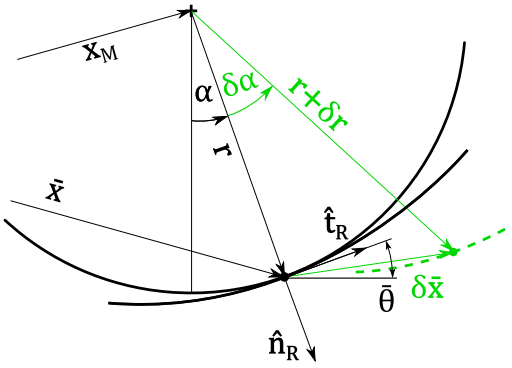

Figure 4: Virtual variation of a contact point

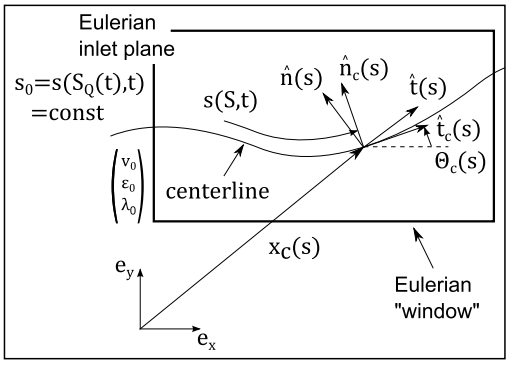

Figure 5: Bending-line and *Eulerian* "window"

$s = s(t, S)$, where the *Eulerian* arc length of the bending-line (i.e. centerline) is denoted by s and the *Lagrangian* "particle name" is denoted by S. To combine advantages of both formulations, an intermediate formulation based on ALE concepts [9] was applied here as well, as it enables a more efficient description of the unterlying hot levelling process.

As proposed already earlier in [7], a referential ALE-coordinate χ is introduced according to

$$\chi = \chi(t, S) = S - S_Q(t) \tag{1}$$

which expresses a "particle name difference" between the *Lagrangian* particle name S and the name of the material particle just moving through the *Eulerian* input plane at time t (cp. Figure 5). This relation yields the differential mapping from *Lagrangian* to ALE domain

$$\mathrm{d}\chi = \mathrm{d}S\,, \quad \mathrm{d}\dot{\chi} = \mathrm{d}\dot{S} = 0\,, \tag{2}$$

while a differential mapping from the *Lagrangian* to the *Eulerian* domain at time t is given by the "axial stretch" $\lambda_c(t, S)$ (index c indicates the centerline)

$$\mathrm{d}s = \lambda_c\ \mathrm{d}S \Leftrightarrow \lambda_c := \frac{\mathrm{d}s}{\mathrm{d}S}\,. \tag{3}$$

By considering the material time derivative of the *Eulerian* arc length increment $\mathrm{d}s$, a strain rate $\dot{\varepsilon}_c$ for the bending-line is introduced.

$$\mathrm{d}\dot{s} = \dot{\lambda}_c\ \mathrm{d}S + \lambda_c\ \mathrm{d}\dot{S} = \frac{\dot{\lambda}_c}{\lambda_c}\ \mathrm{d}s \equiv \dot{\varepsilon}_c\ \mathrm{d}s \tag{4}$$

Integration of (4) yields a logarithmic strain measure of the bending-line.

$$\mathrm{d}\varepsilon_c = \frac{1}{\lambda_c}\,\mathrm{d}\lambda_c \rightarrow \varepsilon_c(s) = \varepsilon_0 + \ln\left[\frac{\lambda_c(s)}{\lambda_c}\right] \tag{5}$$

For arbitrary physical properties described by a field distribution f, the material time derivative $\dot{f}$ can be represented in all three frames of reference as follows:

$$\dot{f} = \frac{\mathrm{d}}{\mathrm{d}t} f^E(s,t) = \frac{\mathrm{D}}{\mathrm{D}t} f^{ALE}(\chi,t) = \frac{\partial}{\partial t} f^L(S,t) \tag{6}$$

where the corresponding operators of the material time derivative take the form

$$\textit{Eulerian:}\ \frac{\mathrm{d}}{\mathrm{d}t} = \dot{s}\,\frac{\partial}{\partial s} + \left.\frac{\partial}{\partial t}\right|_s \quad \text{ALE:}\ \frac{\mathrm{D}}{\mathrm{D}t} = \dot{\chi}\,\frac{\partial}{\partial \chi} + \left.\frac{\partial}{\partial t}\right|_\chi \quad \textit{Lagrangian:}\ \frac{\partial}{\partial t} = \left.\frac{\partial}{\partial t}\right|_S \tag{7}$$

Note that in the *Lagrangian* frame of reference the partial time derivative is already the material one. It can be shown that for the special steady state scenario, where both f^E and f^{ALE} do not depend explicitly on time, the ALE-mesh velocity vanishes identically and the relation $\dot{s} = \lambda_c\,\dot{\chi}$ between $\dot{s}$ and the ALE coordinate-rate $\dot{\chi} = -\dot{S}_Q$ holds. For the special case, where the arbitrary physical property f is identified by the center-line geometry vector $\boldsymbol{x}_c(s)$, the corresponding velocity field distribution is given by

$$\boldsymbol{v}_c(s) = \dot{\boldsymbol{x}}_c(s) = \dot{s}\,\frac{\partial \boldsymbol{x}_c(s)}{\partial s} = \dot{s}\,\hat{\boldsymbol{t}}_c(s) \tag{8}$$

Hence, in a steady state, material particles always move in tangential direction of the bending-line, i.e. the bending-line represents a streamline of material particles. The absolute value of the velocity is then given by

$$v_c(s) = \left\|\boldsymbol{v}_c(s)\right\| = \dot{s}\,. \tag{9}$$

A detailed analysis of the velocity increment with $\mathrm{d}\boldsymbol{x}_c = \hat{\boldsymbol{t}}_c\,\mathrm{d}s$

$$\mathrm{d}\boldsymbol{v}_c(s) = \frac{\mathrm{d}}{\mathrm{d}t}\left(\mathrm{d}\boldsymbol{x}_c(s)\right) \Rightarrow \frac{\mathrm{d}\boldsymbol{v}_c(s)}{\mathrm{d}s} = v_c\,\hat{\boldsymbol{t}}_c' + v_c\,\varepsilon_c'\,\hat{\boldsymbol{t}}_c \tag{10}$$

taking into account the spatial derivative of velocity $\boldsymbol{v}_c(s)$ with respect to the arc length

$$\frac{\mathrm{d}\boldsymbol{v}_c(s)}{\mathrm{d}s} = \frac{\mathrm{d}}{\mathrm{d}s}\left(v_c\,\hat{\boldsymbol{t}}_c\right) = v_c\,\hat{\boldsymbol{t}}_c' + v_c'\,\hat{\boldsymbol{t}}_c \tag{11}$$

immediately yields a relation between the logarithmic (i.e. "true") centerline strain measure ε_c and the corresponding (absolute value of the) bending-line velocity.

$$\mathrm{d}\varepsilon_c = \frac{1}{v_c}\,\mathrm{d}v_c \Rightarrow \varepsilon_c(s) = \varepsilon_0 + \ln\left[\frac{v_c(s)}{v_0}\right] \tag{12}$$

Moreover, by taking into account (12) and (5), a relation between the bending-line velocity v_c and the corresponding axial stretch λ_c is given by

$$v_c(s) = \frac{v_0}{\lambda_0}\,\lambda_c(s), \tag{13}$$

thus, finally a set of closed interrelations between kinematic quantities is obtained.

$$\varepsilon_c(s) = \varepsilon_0 + \ln\left[\frac{v_c(s)}{v_0}\right] = \varepsilon_0 + \ln\left[\frac{\lambda_c(s)}{\lambda_c}\right] \tag{14a}$$

$$v_c(s) = v_0\, e^{\varepsilon_c(s)-\varepsilon_0} = \frac{v_0}{\lambda_0}\,\lambda_c(s), \tag{14b}$$

$$\lambda_c(s) = \lambda_0\, e^{\varepsilon_c(s)-\varepsilon_0} = \frac{\lambda_0}{v_0}\,v_c(s) \tag{14c}$$

6 HIERARCHICAL BEAM MODELS

Extensive *Abaqus*™ simulations of the hot levelling process pointed out that the underlying assumptions within the frame of *Bernoulli-Euler* beam theory are too restrictive for many cases considered, in particular of thick plate. The assumption that cross sectional planes of material particles, which are originally normal to the longitudinal beam axis, i.e. the bending-line, remain normal to it throughout the whole deformation process, is severely violated with increasing plate thickness.

Classical *Timoshenko* beam geometry is based on the description of the bending-line $\boldsymbol{x}_c(s)$ in conjunction with a thickness parameter $h \in \left[-\frac{H}{2}, \frac{H}{2}\right]$ towards an unit vector $\hat{\boldsymbol{n}}(s)$ that includes an angle $\gamma + \frac{\pi}{2}$ (shear deformation γ) with the unit tangent vector $\hat{\boldsymbol{t}}_c(s) = \boldsymbol{x}_c'(s)$ of the bending-line, which according to Figure 5 reads in *Eulerian* representation:

$$\boldsymbol{x}(s,h) = \boldsymbol{x}_c(s) + h \cdot \hat{\boldsymbol{n}}(s)\,. \tag{15}$$

The underlying field variables, leading to degrees of freedom in a discretised model, are the curvature distribution $\kappa(s)$, the bending-line strain $\varepsilon_c(s)$ as well as the shear deformation $\gamma(s)$. The virtual strain energy occurring in the principle of virtual work takes the form

$$\delta W = \int_V \delta\boldsymbol{\varepsilon} : \boldsymbol{\sigma}\ \mathrm{d}V = \int_L \left[\delta\varepsilon_c(s)\cdot N(s) + \delta\kappa(s)\cdot M(s) + \delta\gamma(s)\cdot Q(s)\right]\ \mathrm{d}s\,, \tag{16}$$

where the virtual quantities of the independent field variables, as introduced above, appear beside the corresponding section forces. Herein $N(s)$ denotes the tensile force, stretching the bending-line, $M(s)$ is the bending moment and $Q(s)$ means the transverse shear force.

Neglecting the shearing strain, i.e. $\gamma \equiv 0$, leads to the *Bernoulli-Euler* orthogonality condition. Hence, unit vector $\hat{\boldsymbol{n}}(s)$, which is coinciding with unit normal vector $\hat{\boldsymbol{n}}_c(s)$ of the bending-line is perpendicular to $\hat{\boldsymbol{t}}_c(s)$ and the variational equation (16) reduces analogously. Within the frame of a systematic model reduction, an additional simplification

is obtained by the assumption of neglecting axial stretch, i.e. $\lambda_c(s) \equiv 1$. In this simple case, the only unknown field variable remaining is the bending-line curvature distribution $\kappa_c(s)$ and consequently only the variation $\delta\kappa_c$ of beam curvature remains present in the variational equation.

7 CONTACT FORMULATION

The previous section dealt with variational formulations of different granularity, all of which can be described by applying the principle of virtual work where δW denotes the virtual internal strain energy, whereas the virtual work of external forces is given by δW_s.

$$\begin{aligned} \delta W - \delta W_S &= 0 \\ \delta W_S = \oiint_{\partial V} \left(\delta \boldsymbol{u}^T \, \boldsymbol{\sigma} \, \hat{\boldsymbol{N}}\right) \mathrm{d}S &\longrightarrow \sum_{i=1}^{n_R} \left(\delta r_i \, F_{N,i} + r_i \, \delta\alpha_i \, F_{T,i}\right) \end{aligned} \tag{17}$$

External body forces are neglected in this study, therefore, only surface tractions $\boldsymbol{\sigma}\,\hat{\boldsymbol{N}}$ contribute to δW_s. Both the normal and tangential contact forces, the contributions of which to the virtual work is determined by evaluating a surface integral along the edges of the plate's longitudinal section. In a discretised model, these integral expressions reduce to a sum of n_R concentrated load-vectors acting on each particular levelling roll and consisting of components $F_{N,i}$ in normal and $F_{T,i}$ in tangential direction, respectively.

As is well known [9], contact and friction can be treated very effectively by employing *Lagrange* parameters, leading to additional d.o.f. In this context, per contact node two *Lagrange* multipliers $\lambda_{r,i}$ and $\lambda_{\alpha,i}$ occur, treating the penetration-constraint in radial direction, and a directional constraint in tangential direction, respectively. The interpenetration-constraint between the plate's bending-line and the respective roll center is based on evaluation of the shortest distance between these two bodies and is evaluated by a distance function $r_i := \left\|\boldsymbol{x}_c(s_i) - \boldsymbol{x}_{M,i}\right\|$ that is used to define a non-penetration constraint in radial roll direction as

$$\mathfrak{R}_{r,i} := r_i - R^* = 0\,, \tag{18}$$

with an effective radius $R^* = R + \frac{H}{2}$. The second (tangential) geometric constraint ensures pure tangential contact between the plate and the respective levelling roll, i.e. the tangential vector $\hat{\boldsymbol{t}}_c$ of the bending-line and outward normal vector $\hat{\boldsymbol{n}}_{R,i}$ (cp. Figure 4, also for the definition of the contact angle $\bar{\theta}$) of the ith levelling roll have to be perpendicular to each other.

$$\mathfrak{R}_{\alpha,i} := \hat{\boldsymbol{t}}_c(s) \cdot \hat{\boldsymbol{n}}_{R,i}(\alpha_i) = \sin\left[\alpha_i - (-1)^i \, \bar{\theta}\right] = 0 \tag{19}$$

Taking these constraints into consideration within the frame of virtual work, the respective variational form follows from (18) and (19), respectively, as

$$\begin{aligned} \delta\mathfrak{R}_{r,i} &= \delta r_i \\ \delta\mathfrak{R}_{\alpha,i} &= \delta\alpha_i\,. \end{aligned} \tag{20}$$

The virtual quantities δr_i and $\delta\alpha_i$ involved represent the variation of a contact point $\bar{\boldsymbol{x}} \rightarrow \bar{\boldsymbol{x}} + \delta\bar{\boldsymbol{x}}$ in a polar coordinate system of a levelling roll, as shown in Figure 4.

The relevant variational expression forming the basis of the implemented contact-algorithm, can be summarized as:

$$\delta\left(W_S + \boldsymbol{\lambda}^T \cdot \boldsymbol{\mathfrak{R}}\right) = \sum_{i=1}^{n_R}\left[\delta r_i\,\lambda_{r,i} + \delta\alpha_i\left(r_i\,F_{T,i} + \lambda_{\alpha,i}\right) + \delta\lambda_{r,i}\,\mathfrak{R}_{r,i} + \delta\lambda_{\alpha,i}\,\mathfrak{R}_{\alpha,i}\right] \tag{21}$$

8 SELECTED RESULTS

Several reference simulations were carried out by utilising the *Abaqus*™ model for plate thicknesses $H = \{10,\ 20,\ 30,\ 50\}$ mm. So far attained solutions comprised essential quantities, such as curvature values associated with mesh nodal coordinates and vertical levelling force-values. These results can be considered a reference for solutions of a taylor-made software prototype developed according to the concepts outlined in Sections 4–7. The numerical solution algorithm is based on a damped variant of *Newton*'s method and is implemented in C++. For each thickness value, multiple simulations were performed with different element node distributions, i.e. both the number and the mesh density were varied systematically. A perfectly rigid levelling machine was assumed in these simulations to verify the validity of the self-made prototype compared to *Abaqus*™.

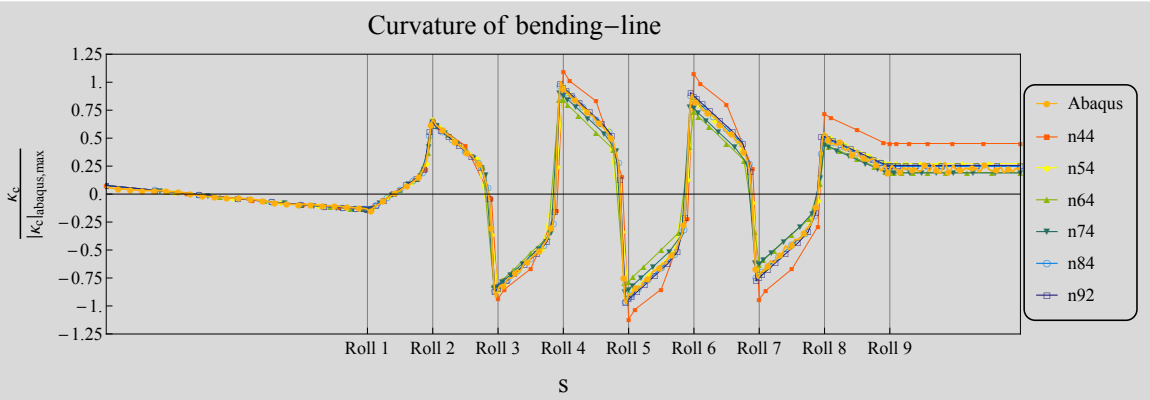

Figure 6: Curvature of bending-line for plate with $H = 20\,\text{mm}$

An analysis of simulation results including the elastic machine deformation led to significant changes in plate curvature as well as levelling forces due to non-neglectable vertical levelling roll-center displacements. The results presented in Section 8.2 exhibit significant differences especially for thick plates, when comparing solutions obtained with and without elastic machine deflection under load.

8.1 Rigid Machine Model

Curvature-values at the element nodes, together with the involved contact *Lagrange* multipliers, represent the numerical solution of the simplest levelling process model under consideration (cp. Section 6). Integrating twice along the curvature distribution yields the

bending-line of the plate, whereas the *Lagrange* parameters represent contact forces and hence levelling forces acting on the respective levelling rolls. The curvature distribution of a plate with thickness $H = 20\,\text{mm}$, as shown in Figure 6 are relative values referred to the largest curvature occurring in the referential *Abaqus*™ solution. An suitable input parameter set of `gap`, `skew`, and levelling `speed` values was assumed, leading to about 80 % cross sectional plastification. It can be seen that the results obtained from the self-developed software prototype seem to converge satisfactorily to the referential *Abaqus*™ solution when the number of elements is increased. While the shape of the curvature distribution corresponding to $n_{el} = 44$ elements still displays significant deviations, simulations with finer mesh resolutions, $n_{el} = 84$ and $n_{el} = 92$, respectively, exhibit almost no deviation from the reference curve on the scale of Figure 6. Residual plate curvature was not reduced to a very low value with the chosen input parameters, hence, the resulting plate remains (almost) uniformly curved.

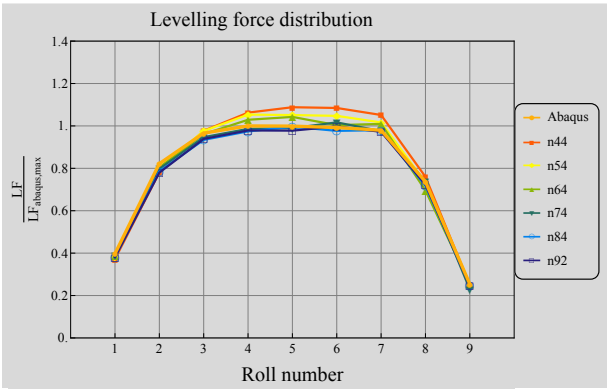

Figure 7: Levelling forces for plate with $H = 20\,\text{mm}$

Levelling forces resulting from the self-developed software prototype approximate the *Abaqus*™ results from above better and better with increasing mesh density, as can be seen from Figure 7. For element numbers $n_{elem} \geq 74$ (i.e. $n74$, $n84$, $n92$), there are only minor differences compared to the *Abaqus*™ reference solution. It should be mentioned that a general tendency to slightly smaller values in levelling forces can be observed for the self-developed software prototype.

8.2 Deformable Machine Model

For this realistic modelling scenario, two selected simulations are presented, namely for plate thickness values of $H = 10\,\text{mm}$ and $H = 50\,\text{mm}$, respectively, to display the influence of the machine deformation on curvature and bending-line distributions, as well as feedback effects on corresponding levelling forces.

The elastic machine deflection, i.e. the upper vertical roll-center displacements, is relevant even for thin plates, but as can be seen from Figure 8, it just takes an elastic deflection value of 0.12 mm compared to an unloaded position set-up (prescribed `gap`, `skew`) of 21 mm at this roll. Therefore, elastic deformation only slightly influences the resulting curvature and levelling force distribution. Figure 9 shows the local relative change of levelling forces with respect to vertical roll displacements due to machine deformation. Compared to the ideal case of a fully rigid machine, forces take slightly smaller values. The same holds true for the total levelling force that decreases marginally by about 0.15 %.

The observed changes for the thick plate appear more drastic, as can be seen in Figure 10. The upward roll-center displacement of 2.3 mm, compared to a position-setup of

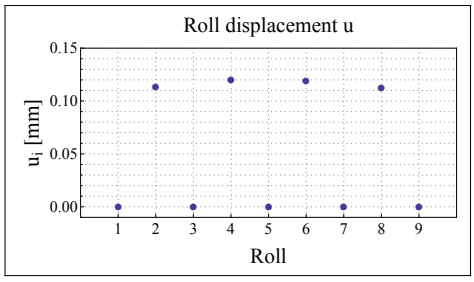

Figure 8: Impact of machine deformation on roll positions for thin plate ($H = 10\,\text{mm}$)

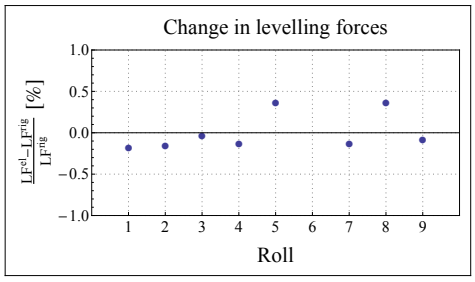

Figure 9: Impact of machine deformation on levelling forces for thin plate ($H = 10\,\text{mm}$)

4.2 mm, means a position-deviation at roll 2 by more than 50 % and the same holds true at the other upper rolls. This relatively high change of the loaded levelling gap has a direct impact on the cross sectional plastification, which is significantly reduced from about 75 % in the rigid case to about 55 %, when elastic roll deflection is considered. However, for a perfectly rigid levelling machine, plastic plate deformation may in general occur at each levelling roll. For the levelling scenario under consideration, almost no plastic deformation occurs at roll 5, and it completly vanishes downstream. The elastic machine deformation

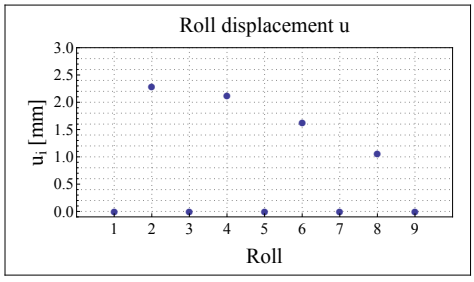

Figure 10: Impact of machine deformation on roll positions for thick plate ($H = 50\,\text{mm}$)

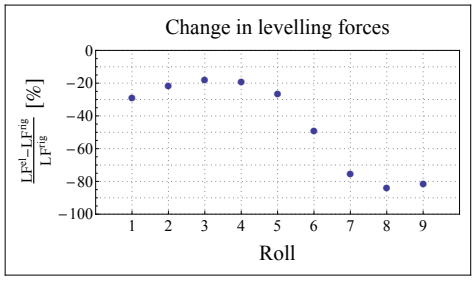

Figure 11: Impact of machine deformation on levelling forces for thick plate ($H = 50\,\text{mm}$)

significantly affects the levelling forces, as is shown in Figure 11, where forces up to roll 5 change moderately between −20 % and −30 % whereas the tiny forces at the levelling rolls near exit (cp. Figure 7) change by a total of up to −85 %.

9 CONCLUSIONS

Comprehensive knowledge of detailed physical effects and the influence of process parameters on the properties of hot and cold levelled heavy plate was acquired by performing extensive parameter studies with the commercial FEM-package *Abaqus*™, the results of which formed the basis for the development of taylor-made numerical simulation prototypes of different granularity. All model prototypes under consideration are based on the principle of virtual work and appropriate ALE formulations for 2D beam elements. Contact and friction turned out to be extremely crucial in this context and were treated consistently by employing *Lagrange* parameters. Systematic process analyses point out the importance to include machine deformation when dealing with hot levelling processes.

The presented model is already in use for offline parameter studies. The next development step comprises the accomplishment of process models for online purposes. In combination with adequate numerical tools calculating the flow curve of the processed material, based on the current state (thickness distribution of both temperature and state of phase transformation), set-up values of gap and skew can be determined precisely with the new generation of the automation system for the hot and cold levelling machines. Besides, these modeling concepts form the basis to develop enhanced simulation prototypes incorporating shear deformable beam theory to meet the challenges occurring especially when dealing with thick heavy plate.

ACKNOWLEDGEMENT

This work has been supported by the Austrian COMET-K2 programme of the Linz Center of Mechatronics (LCM) in cooperation with *voestalpine Grobblech GmbH*, and has been funded by the Austrian federal government and the federal state of Upper Austria.

REFERENCES

[1] Geleji, A. *Die Berechnung der Kräfte und des Arbeitsbedarfs bei der Formgebung im bildsamen Zustand der Metalle.* Akademia Kiado Budapest, (1955).

[2] Batty, F.A. and Lawson, K.T. Heavy Plate Leveller. *Iron- and Steelworks Engineering* (1955) 1115–1128.

[3] Thiele, H. *Untersuchungen über das Richten und Walken von Bändern.* PhD Thesis, Technische Universität Berlin, (1970).

[4] Ploetz, K. *Ein Beitrag zum Biegerichten von rand- und mittenwelligen Blechen in Richtmaschinen.* PhD Thesis, Montanistische Hochschule Leoben, (1973).

[5] Witte, H.-D. *Untersuchung über das Walzrichten von Metallbändern mit symmetrisch angestellter Fünf-Walzen-Richtmaschine.* PhD Thesis, Universität Stuttgart, (1970).

[6] Finstermann, G. *Rechnerische Simulation des Biegerichtens gebeulter Bleche und Bänder.* Montanistische Hochschule Leoben, (1989).

[7] Steinwender, L., Kainz, A., Krimpelstätter K. and Zeman, K. An Arbitrary Lagrangian-Eulerian (ALE) Approach for the Modelling of Tension Levelling Processes. *Computational Plasticity XI - Fundamentals and Applications* (2011).

[8] Baumgart, M., Steinböck, A., Kugi, A., Douanne, B., Raffin-Peyloz, G., Irastorza, L. and Kiefer, T. Modeling and Active Compensation of the Compliance of a Hot Leveler. *Steel Research International 2011, Special Edition* (2011) 337–342.

[9] Belytschko, T., Liu, W.K. and Moran B., *Nonlinear Finite Elements for Continua and Structures.* John Wiley & Sons Ltd., (2000).